ACS APPLIED MATERIALS & INTERFACES
Research Article
www.acsami.org

Reversible Quenching of a Chromophore Luminescence by Color Transition of a Polydiacetylene

Thierry Barisien,*,† Jean-Louis Fave,† Sophie Hameau,† Laurent Legrand,† Michel Schott,† Jeremy Malinge,‡ Gilles Clavier,‡ Pierre Audebert,‡ and Clémence Allain*,‡

†Institut des NanoSciences de Paris (INSP), UPMC Université Paris 6 - CNRS, UMR7588, 4 place Jussieu, 75252 Paris cedex 05, France

‡PPSM, CNRS UMR8531, Ecole Normale Supérieure de Cachan, 61 avenue du Président Wilson, 94235 Cachan cedex, France

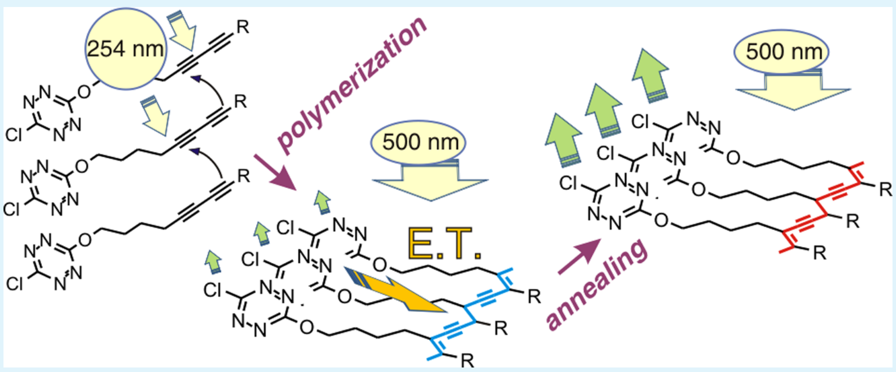

ABSTRACT: A new reactive diacetylene molecule has been synthesized, incorporating a strongly luminescent chromophore, tetrazine (Tz). It readily polymerizes into the blue polydiacetylene (PDA) form, quenching the Tz luminescence already at concentrations ≤1 %. The blue to red PDA transition is thermally induced in the solid state and the original strong Tz emission is restored. This might lead to a new type of detection for sensors using the PDA color transition.

KEYWORDS: *chromatic transition, sensors, polydiacetylene, energy transfer, tetrazine*

1. INTRODUCTION

There is currently a large research activity on the development of biological and chemical sensors using molecular films or vesicles containing polydiacetylenes (PDA). The detection scheme uses the so-called "color transition" of PDA: these polymers exist in two forms, so-called "red" and "blue", which correspond to different chain conformations.[1] Typical absorption spectra before and after a blue to red transition are shown on Figure 1. The chosen PDA in this figure is pentacosadiynoic acid for two reasons: it is a clear cut case and the material or its derivatives have been very often used in the design of film or vesicle sensors using PDA.

The principle of these sensors is that a small fraction of the diacetylene monomers in the film or vesicle are functionalized at their outer end with a chemical group having a specific affinity for what is to be detected (molecule, ion, biological polymer, virus coat protein, etc.). In some cases, an amphiphilic molecule is simply mixed with the DA monomers.[2] Binding triggers the color transition, through a mechanism that is not yet well understood. Initially, sensors used the absorption change, following the pioneering work by the group of Charych.[3] However, using fluorescence would be more advantageous, particularly in terms of sensitivity, if sensor action turns the emission on.[2,4,5] Recently, chromophores have been incorporated in films or vesicles with the aim of using energy transfer between them and PDA chains.[6]

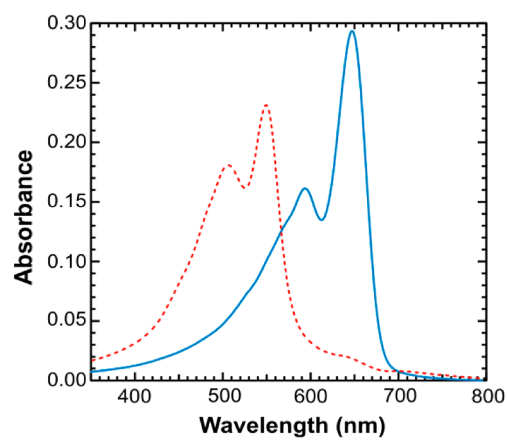

Figure 1. Absorption spectra of a polymerized pentacosadiynoic thin polycrystalline film before (blue continuous line) and after (red dashed line) the thermally produced color transition.

Received: July 26, 2013
Accepted: October 8, 2013
Published: October 8, 2013

   dx.doi.org/10.1021/am403039u | ACS Appl. Mater. Interfaces 2013, 5, 10836−10841

In this work, we present a model system, which geometry can be exactly known, where the energy transfer characteristics are the same for all molecules and the polymer content can be measured and controlled. The final aim will be to reach thorough understanding of the process at play. The chromophore emission is the signal of interest and is driven uniquely by the specific interaction the chromophore has with each of the blue or red structure of the PDA conjugated backbone. To do so, the chromophore is covalently attached to the diacetylene (DA) group, instead of being mixed in the film or vesicle with DA monomers as separate molecules, so any segregation is avoided. The PDA-chromophore interaction is strong and the same for all molecules. The proposed process also differs from most previous ones in another important feature: the detection is performed by the chromophore fluorescence which may be much more intense than that of the red PDA (in this work by a factor larger than 10). The chosen chromophore must be able to transfer its energy to the blue chains, but not to the red ones. In addition it should not interfere with the topochemical conditions for the polymerization reaction. Therefore, the smallest possible chromophore was chosen, tetrazine[7] (Tz), the absorption and emission bands of which also meet requirements and allow appropriate energy transfers.

To the best of our knowledge, there is a single example of a similar process described in the literature where the manipulation of luminescence through Förster resonance energy transfer (FRET) is achieved between a covalently attached chromophore and the PDA isomeric forms.[8,9] A significant difference however exists between the work in[8] and the present approach: here, the geometry defining the Tz-DA arrangement is well-determined and invariable for every Tz-DA pairs. In other papers reporting about chromatic transition-based sensors, different schemes are at play. For instance, in the "on" state, the chromophore (donor) assembly (attached to the DA or not) harvests energy and transfers it to the red luminescent PDA structure, leading to amplified PDA emission.[10−12] FRET can also be modulated by structural rearrangement, through modification of the donor−acceptor distance but the chromatic transition is not necessarily responsible for the variations in the donor−acceptor coupling.[13]

Here we study the commutation between emissive and nonemissive states of the Tz chromophore, exclusively induced by the PDA electronic phase transition. Energy transfers are studied in thin polycrystalline films so that the process potentiality can be explored in a well-defined frame where structural disorganization, often at play in vesicle sensors, is minimized.

Note also that the present note provides a proof of principle of a general scheme, but it was not our intention at this stage to prepare an actual sensor nor do we claim that the molecule used here will itself provide a sensor.

2. EXPERIMENTAL SECTION

2.1. Materials. All chemical reagents and solvents were purchased from commercial sources (Aldrich, Acros, SDS) and used as received. Analytical TLC was performed on Kieselgel F254 precoated plates. Visualization was done with UV lamp. Flash chromatography was carried out with silica gel 60 (230-400 mesh) from SDS. Melting points were determined on a capillary melting point apparatus and are uncorrected. ^{1}H and ^{13}C NMR spectra were recorded on a JEOL 400 MHz spectrometer, and chemical shifts (δ) were reported in ppm relative to TMS and referenced to the residual solvent. Coupling constants (J) are reported in Hz and refer to apparent peak multiplicities. Multiplicities are reported using the following abbreviations: s, singlet; d, doublet; t, triplet; q, quadruplet ; m, multiplet; bs, broad singlet. High-resolution mass spectra were performed at ICSN (Imagif platform, CNRS, Gif-sur-Yvette, France).

3,6-dichloro-s-tetrazine[14] and 6-bromo-hexyn-5-ol[15] were prepared according to literature procedures.

Hex-5-ynyl Butoxycarbonylmethylcarbamate **2**. A solution of 5-hexyn-1-ol (1.50 g, 15.3 mmol), triethylamine (1.70 g, 16.8 mmol) and butylisocyanatoacetate (2.64 g, 16.8 mmol) in toluene (50 mL) was refluxed for 17 h. The reaction mixture was cooled down to room temperature, washed with brine (3x25 mL) and dried on magnesium sulfate. The crude product was purified by chromatography on silica gel (elution with petroleum ether/ethyl acetate 7/3) to afford **2** as a colorless oil, with a quantitative yield.

^{1}H NMR (400 MHz, $CDCl_3$): δ =5.23 (br s, 1H, NH), 4.18-4.08 (m, 4H), 3.96 (d, J = 5.5 Hz, 2H), 2.24 (td, J = 7.3 Hz, J = 2.8 Hz, 2H), 1.96 (t, J = 2.8 Hz, 1H), 1.78-1.69 (m, 2H), 1.67-1.56 (m, 4H), 1.43-1.33 (m, 2H), 0.93 (t, J = 7.3 Hz, 3H) ppm.

^{13}C NMR (100 MHz, $CDCl_3$): δ =170.3, 156.6, 84.0, 68.8, 65.4, 64.8, 42.8, 30.6, 28.1, 24.9, 19.1, 18.2, 13.7 ppm.

12-Hydroxydodeca-5,7-diynyl Butoxycarbonylmethylcarbamate **3**. A mixture of CuCl (0.146 g, 1.47 mmol), n-butylamine (5.8 mL, 58.8 mmol), water (30 mL), CH_2Cl_2 (30 mL) and **2** (1.50 g, 5.88 mmol) at 0°C was treated with hydroxylamine hydrochloride until decoloration. 6-bromohex-5-yn-1-ol (1.04 g, 5.88 mmol) dissolved in CH_2Cl_2 (10 mL) was then added dropwise. Few crystals of hydroxylamine may be needed to prevent the reaction from turning green. The reaction mixture was stirred overnight under Ar. The organic layer was then extracted with CH_2Cl_2 (30 mL), washed with saturated aqueous ammonium chloride (4 × 30 mL), dried over $MgSO_4$, and concentrated in vacuo. The residue was then purified over silica (gradient from 20 to 50% ethyl acetate in petroleum ether) providing **3** as a colorless oil (1.66 g, 80% yield).

^{1}H NMR (400 MHz, $CDCl_3$): δ = 5.21 (br s, 1H, NH), 4.15-4.06 (m, 4H), 3.93 (d, J = 5.5 Hz, 2H), 3.64 (t, J = 6.2 Hz, 2H), 2.28 (t, J = 6.8 Hz, 2H), 2.27 (t, J = 6.8 Hz, 2H), 1.76-1.52 (m, 10H), 1.41-1.31 (m, 2H), 0.91 (t, J = 7.3 Hz, 3H) ppm.

^{13}C NMR (100 MHz, $CDCl_3$): δ =170.3, 156.6, 77.4, 65.8, 65.6, 65.4, 64.8, 62.3, 42.8, 31.8, 30.6, 28.1, 24.8, 24.7, 19.10, 19.06, 18.9, 13.7 ppm.

Monomer **1**. To a stirring solution of **3** (0.70 g, 2.0 mmol) in dry CH_2Cl_2 (20 mL) were successively added dichlorotetrazine (0.33 g, 2.2 mmol) and 2,4,6-collidine (0.29 mL, 2.2 mmol). The resulting mixture was stirred at room temperature for 4 h. The mixture then was concentrated and the residue was purified over silica gel (30 % EtOAc in petroleum ether), providing the desired product as a fluorescent solid (0.61 g, 65 %), which should be cautiously protected from light.

^{1}H NMR (400 MHz, $CDCl_3$): δ = 5.21 (br s, 1H, NH), 4.68 (t, J = 6.4 Hz, 2H), 4.15 (t, J = 6.6 Hz, 2H), 4.11 (t, J = 6.4 Hz, 2H), 3.96 (d, J = 5.5 Hz, 2H), 2.38 (t, J = 6.9 Hz, 2H), 2.30 (t, J = 6.9 Hz, 2H), 2.10−2.02 (m, 2H), 1.80−1.69 (m, 4H), 1.64-1.54 (m, 4H), 1.43−1.33 (m, 2H), 0.93 (t, J = 7.3 Hz, 3H) ppm.

^{13}C NMR (100 MHz, $CDCl_3$): δ = 170.3, 166.7, 164.4, 156.5, 77.3, 76.5, 70.4, 66.2, 65.6, 65.5, 64.8, 42.8, 30.6, 28.1, 27.6, 24.8, 24.5, 19.1, 18.95, 18.91, 13.8 ppm.

ESI-MS: 466.2 ([M + H+], 100 %), 488.2 [M+Na+], 70 %), 953.3 [2M + Na+], 35 %), HRMS: calcd for $C_{21}H_{29}ClN_5O_5$, 466.1857; found, 466.1856 (−0.2 ppm).

2.2. Elaboration of Thin Films. Thin films were prepared by melting a small amount (less than 1 mg) of pure monomer **1** between two glass or SiO_2 plates. The cover plate protects the Tz and the formed PDA from photooxidation. These films are polycrystalline with typical crystal sizes between 10 and 100 μm (as shown on Figure 2), and typically 1−10 μm thick. Photopolymerization was performed by short (up to 5 min) UV irradiations in the range 230−270 nm where monomer DA absorbs,[16] using a 150 W Xe lamp (Spectra Physics) and a dielectric mirror reflecting unpolarized light in the chosen range (Melles-Griot KRF-2037-45-UNP). The color transition was achieved by annealing the film to 60°C, below its melting point.

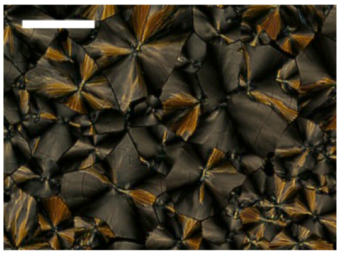

Figure 2. Microscopy view in transmission, and between crossed polarizers, of a thin film made of monomer **1**. The bar in the image represents 50 μm. The films are made of crystalline areas with birefringent activity and sizes up to several tens of micrometers.

2.3. Raman Spectroscopy. Excitation was produced by an He-Neon laser (632.8 nm) or by an Argon laser (Coherent Innova 90) pumping a dye laser (Coherent CR99) using Rhodamine 6G dye. In the latter case continuous range of wavelengths from 560 to 585 nm can be obtained. The signal is dispersed in a double monochromator (Jobin Yvon Ramanor U1000) and detected by a cooled RCA C31034 photomultiplier. The obtained spectral resolution is ~2 cm^{-1}. The laser beam on the sample is focused thanks to a cylindrical lens leading to a spatial extension of the beam of about 1.5 mm laterally and a fraction of millimeter in height to minimize the photon flux.

2.4. Photoluminescence and Absorption Measurements. Absorption spectra were recorded using a Cary 5000 (Varian) double beam spectrophotometer. Tetrazine emission was excited at 337 nm by a N_2 laser (LTB MNL200) or directly in the tetrazine absorption range by green laser emission from selected dyes pumped at 337 nm. Emission spectra and temporal decays were recorded using a Jobin-Yvon TriAx 190 spectrometer with cooled CCD camera and Hamamatsu H6780-01 photomultiplier module feeding a fast homemade amplifier. Decays were averaged with sub-nanosecond resolution in a TDS 5034 Tektronix oscilloscope. With sub-nanosecond laser pulse widths, the overall instrument temporal response was a Gaussian with a fwhm ~3.1 ns. Data were further processed, deconvoluted, and signal to noise ratio at long time enhanced by logarithmic binning. Complete sets of measurements in absorption and emission were obtained for the monomer, after each polymerization step, and after annealing.

3. RESULTS AND DISCUSSION

The monomer used here contains a tetrazine ring, a diacetylene group, and an urethane, with alkyl spacers between them, as shown on Scheme 1 (compound **1**). The urethane is used as an "organizing" group favoring a geometry suitable for the polymerization reaction.[17] Monomer **1** is obtained in three steps from commercially available 5-hexyn-1-ol. In a first step, 5-hexyn-1-ol is reacted with butylisocyanatoacetate to afford the carbamate **2** with a quantitative yield. Cadiot-Chodkiewicz coupling of **2** and 5-bromohexyn-1-ol (synthesized by bromination of 5-hexyn-1-ol with bromine in aqueous KOH)[15] in CH_2Cl_2/water leads to diacetylenic alcohol **3** with a 80% yield. Nucleophilic aromatic substitution of one of the chlorine atoms of 3,6- dichlorotetrazine by diacetylenic alcohol **3**, following a procedure optimized in our group[14] affords monomer **1** with 65% yield.

Scheme 1. Synthesis of Monomer 1

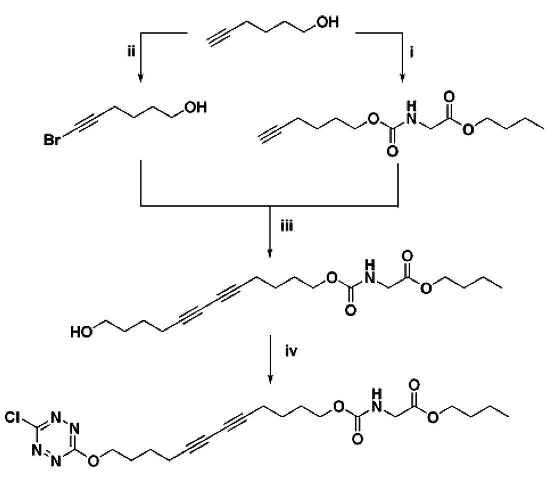

Figure 3a shows a typical absorption spectrum of a c.a. 4 μm thick monomer film. It is dominated by the S_1 and S_2 bands of chloroalkoxytetrazine with maxima near 518 and 320 nm, and the strong increase below 230 nm corresponds to a very intense transition of the tetrazines. But one also sees the weak diacetylene absorption band near 254 nm, the other higher energy ones being buried in the rise of the strong tetrazine absorption near 210 nm.[16] The band near 265 nm corresponds to another weak tetrazine absorption.[14]

The absorbance at 518 nm was used to estimate films thicknesses using the absorbance determined for a very similar monomer, differing from the molecule used here only by being terminated with a propyl group instead of the butyl ester. The absorbance in the UV range used for photopolymerization (230-270 nm) is often high, in which case polymerization will be heterogeneous in depth, and only average polymer contents may be estimated. The absorbance at the luminescence excitation wavelength (337 nm) is higher so only the most polymerized part of the film is probed. The thinnest film prepared by this method had absorbances of ~0.2 and ~0.52 near 250 nm and at 337 nm respectively, corresponding to thickness of ~1 μm, so leading to nearly homogeneous polymerization in depth.

Note that the absorption spectrum of the molecule in n-hexane shows sharper structures making the identification of the 0-0 pure electronic transition possible: $\lambda_0 \approx 550$ nm (see the arrow in the inset of Figure 3a). The Tz-DA monomer transition is thus located at a slightly lower energy than the pure electronic transition of red PDA chains so that energy transfer if occurring will be from the red polymer to the Tz acceptors.

Upon UV irradiation, a new absorption appears and grows up with a maximum near 615 nm as shown on Figure 3b. An obvious assignment is to a growing concentration of PDA chains. This was confirmed by taking a resonance Raman spectrum with 633 nm excitation, to avoid interference by tetrazine emission : all known blue PDA lines are present and only them since the excitation wavelength is far from resonance with the Tz absorption (see Figure 3c). The PDA chains formed absorb at slightly shorter wavelength than standard blue chains, and their characteristic double bond and triple bond stretching frequencies are slightly higher. This may be either because they are slightly strained in tension,[20] or because their geometry is not exactly planar.[1] We shall call them "blue chains". The maximum absorptivity of those PDA chains is not yet known but that of the blue PDA is usually in the range 1 to a few 10^5 cm^{-1}.[21] Using this value leads to a polymer content of the order of ~1% after 5 min of irradiation. After annealing, this absorption has completely disappeared. A difference spectrum (spectrum after annealing minus the spectrum just before) displayed on Figure 3d shows in negative the disappearance of the "blue" absorption and in positive a typical red chains

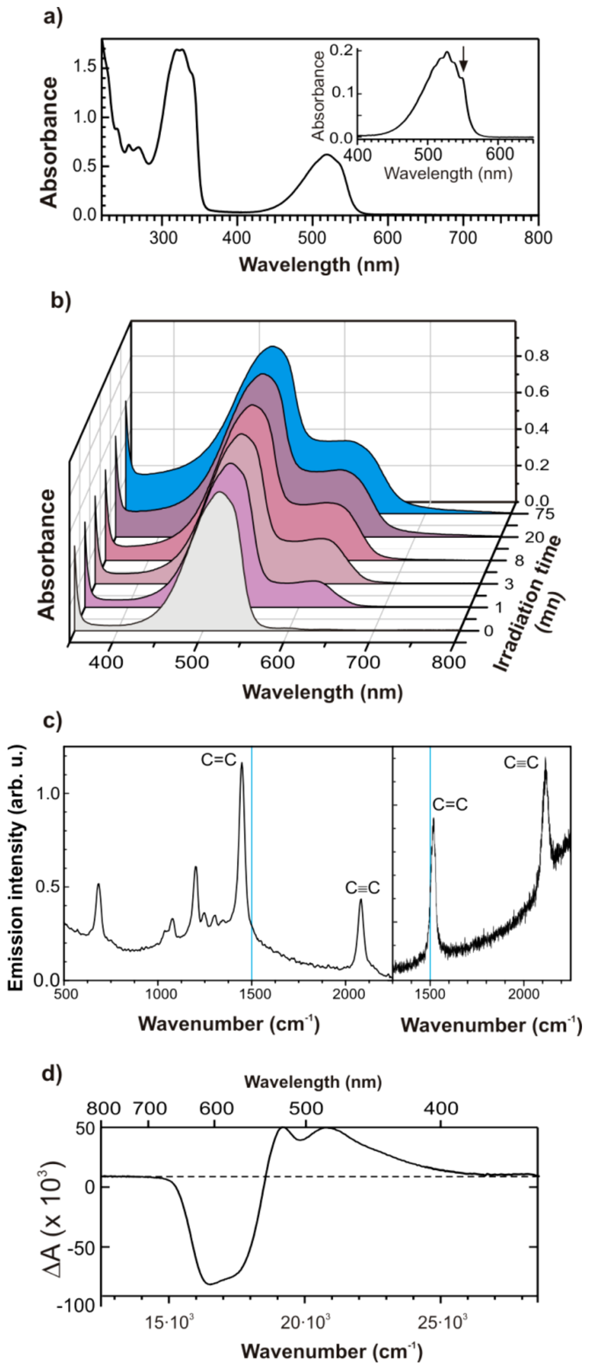

Figure 3. (a) Monomer absorption spectrum in a thin solid film (thickness ≈ 4 μm). Inset: absorption spectrum of the monomer in n-hexane. (b) Absorption spectra as a function of UV irradiation duration from 0 to 75 min in a 5 μm thick film showing the growth of the long wavelength absorption. (c) Left panel: room-temperature Raman spectrum of a monomer **1** irradiated thin film, excited at 632.8 nm (excitation power ≈ 10 mW). The peak of the double bond stretching mode is well-identified and its frequency measured at 1450 ± 2 cm^{-1} (C≡C at 2081 ± 2 cm^{-1}); its presence results from the polymerization reaction and the generation of an enyne chain structure of blue type.[18] Right panel: Raman spectrum of an annealed irradiated film (excitation is the 457.9 nm argon line); the measured frequencies of the double and triple bond modes (1508 ± 1 cm^{-1} and 2115 ± 1 cm^{-1}) now correspond to a red like PDA structure.[19] The underlying broad signal corresponds to the rising higher energy flank of the Tz emission. There is no more signatures of the blue structure in the recorded spectra. (d) Difference of the spectra after and before

Figure 3. continued

annealing on a 1 μm thick film. ΔA is a variation of absorbance. Note that two abscissa have been shown and one is in wavenumbers to allow comparison of the areas under the two parts of the ΔA curve. The inequality between the areas (ratio of ~0.82) may be related to small differences in oscillator strength of the two PDA forms (see also Figure 1). $\Delta A < 0$ indicates the conversion of the blue structure (at lower energy) to the red one ($\Delta A > 0$ at higher energy).

spectrum. This demonstrates the conversion of the blue chains to the red ones. Red chain formation is further confirmed by the shift to higher frequency of each of the C═C and C≡C backbone stretching modes (Figure 3c).

The film emission spectrum is a typical chloroalkoxy tetrazine spectrum[22] (Figure 4). Comparison with difference

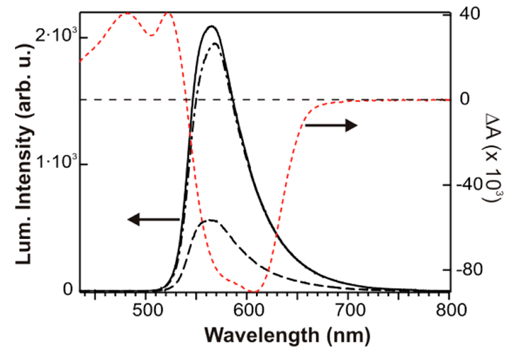

Figure 4. Emission spectrum of the monomer film: before irradiation (solid line), after 5 minutes irradiation (dashed line) and after annealing (dash-dotted line); the red dotted line reproduces the red PDA absorption of Figure 3d (here plotted in wavelength), ΔA is defined in the caption of Figure 3.

spectrum of figure 3d shows that there is very little overlap with the red chains absorption confirming that energy transfer from Tz to the red chains is highly disfavored. DA polymerization leaves the emission spectrum shape unchanged (Figure 4) but the overall intensity decreases considerably. This shows that a blue PDA concentration ≤1 % is enough to quench the tetrazine emission almost completely. However after annealing this intensity is almost completely restored. This shows in addition that no significant tetrazine photolysis has occurred. Typical data are given in Table 1.

Simultaneously, the whole dynamics gets faster upon increasing the polymer content, then is recovered after annealing. The overall decays are complex due to the presence

Table 1. Evolution with Irradiation Time, Of Some Characteristics of the Tz Emission; Absorbance of Formed Blue PDA Chains Is Also Mentioned

	λ_{max} (nm)	I_0 at λ_{max} (arb. u.)	ratio[a]	absorbance at 615 nm[b]
monomer	566	2090	1	0
1 min[c]	566	1127	0.54	0.08
2 min	565	834	0.40	0.14
3 min	565	592	0.28	0.18
5 min	564	561	0.27	0.22
annealed	569	1950	0.93	0

[a]Remaining fraction of the initial intensity. [b]At maximum of blue chain absorption. [c]Irradiation time in minutes.

of delayed fluorescence and will be further analyzed elsewhere. Figure 5 clearly shows the variations in the initial lifetimes.

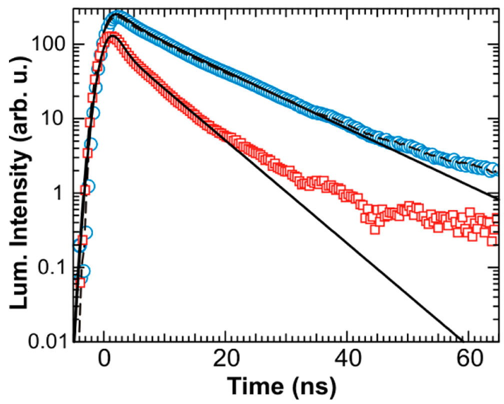

Figure 5. Luminescence decays of a monomer film before irradiation (blue open circles), after 5 min irradiation (red open squares) and after annealing (dashed line). The solid lines are fits obtained taking into account the apparatus response function (see the Experimental Section). The "short time" dynamics over ~30 ns can be adjusted using two decay rates τ_1 and τ_2; at longer time, the decays are no more exponential whatever the polymer content. Before irradiation, τ_1 = 2.4 ns and τ_2 = 11.3 ns; after 5 mn, irradiation τ_1 = 1.0 ns and τ_2 = 6.3 ns. Consecutive annealing leads to a full restoration of the decay.

Note in particular that the decays before irradiation and after annealing are completely superimposed. It is clear that the Tz-polymer coupling opens non-radiative channels that do not affect the overall shape of the decays but manifest itself through a decrease in the luminescence and a pronounced acceleration of the dynamics.

Careful examination of the emission spectra reveals a weak fluorescence peaking at 650 nm after irradiation. This emission band disappears after annealing, so it has to be an emission by the PDA blue chains. It is much weaker than the tetrazine emission, so it can only be seen on difference spectra (Figure 6).

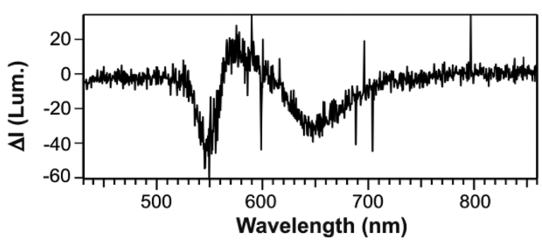

Figure 6. Difference between the emission spectrum after 5 min irradiation and the monomer spectrum (spectra are normalized for $\lambda = \lambda_{max}$ before subtraction). New emission peaking at 650 nm appears negative. The structure below 600 nm (with a "derivative" shape) is due to the small shift of the Tz emission in the irradiated film (see λ_{max} in Table 1).

The blue chains emission quantum yield at room temperature is very low, $\approx 1 \times 10^{-5}$.[23,24] Because direct absorption by PDA chains at 337 nm is very inefficient,[16] this emission must result from the same energy transfer process from the Tz, which accounts for Tz fluorescence quenching. Because the exact fluorescence quantum yield of blue PDA chains in the present material is not known, the number of Tz molecules that funnel their energy towards a PDA chain can only be estimated; a reasonable order of magnitude is 100 molecules, in agreement with the observation that most of the Tz fluorescence is quenched with 1% polymer. Tz molecules in this material harvest energy for the PDA chains.

After the color transition to red chains has been completed, further UV irradiation produces blue chains, while the red ones remain; the new blue chains are produced by further polymerization and not by a photoinduced red to blue transition. These new blue chains can be transformed to red ones by further annealing. After each annealing, the tetrazine emission is recovered, showing that the accumulating red chains do not significantly quench this emission. As a consequence, a sensor built on this principle might be reusable.

4. CONCLUSION

To sum up, we demonstrate that PDA chains absorbing near 615 nm efficiently quench the tetrazine emission. The quenching is no more present after the color transition: Tz fluorescence is fully restored by the blue to red transition. New blue chains can be created and this cycle of quenching and return of fluorescence by annealing can be repeated. These results suggest that this new diacetylene covalently linked to a tetrazine chromophore could open the way to new, well-defined fluorescent sensors based on the PDA chromatic transition.

■ AUTHOR INFORMATION

Corresponding Authors

*E-mail: barisien@insp.jussieu.fr.
*E-mail: clemence.allain@ppsm.ens-cachan.fr.

Author Contributions

The manuscript was written through contributions of all authors. All authors have given approval to the final version of the manuscript.

Notes

The authors declare no competing financial interest.

■ ACKNOWLEDGMENTS

The authors thank the DGA (Direction Générale de l'Armement) for a Ph.D. fellowship to J.M..

■ REFERENCES

(1) Filhol, J.-S.; Deschamps, J.; Dutremez, S.; Boury, B.; Barisien, T.; Legrand, L.; Schott, M. *J. Am. Chem. Soc.* **2009**, *131*, 6976−6988.
(2) Chen, X.; Zhou, G.; Peng, X.; Yoon, J. *Chem. Soc. Rev.* **2012**, *41*, 4610−4630.
(3) Okada, S.; Peng, S.; Spevak, W.; Charych, D. *Acc. Chem. Res.* **1998**, *31*, 229−239.
(4) Reppy, M. A.; Pindzola, B. A. *Chem. Commun.* **2007**, 4317−4338.
(5) Yoon, B.; Lee, S.; Kim, J.-M. *Chem. Soc. Rev.* **2009**, *38*, 1958−1968.
(6) Reppy, M. A. In *Advanced Fluorescence Reporters in Chemistry and Biology II: Molecular Constructions, Polymers and Nanoparticles*; Demchenko, A. P., Ed.; Springer: Berlin, 2010; Vol. 9, pp 357−388.
(7) Clavier, G.; Audebert, P. *Chem. Rev.* **2010**, *110*, 3299−3314.
(8) Dogra, N.; Li, X.; Kohli, P. *Langmuir* **2012**, *28*, 12989−12998.
(9) Li, X.; Kohli, P. *J. Phys. Chem. C* **2010**, *114*, 6255−6264.
(10) Li, X.; McCarroll, M.; Kohli, P. *Langmuir* **2006**, *22*, 8615−8617.
(11) Li, X.; Matthews, S.; Kohli, P. *J. Phys. Chem. B* **2008**, *112*, 13263−13272.
(12) Seo, S.; Kim, D.; Jang, G.; Kim, D.-M.; Kim, D.; Seo, B.-K.; Lee, K.; Lee, T. *Reactive & Functional Polymers* **2013**, *73*, 451−456.
(13) Ma, G.; Müller, A.; Bardeen, C.; Cheng, Q. *Adv. Mater.* **2006**, *18*, 55−60.

(14) Gong, Y.; Miomandre, F.; Méallet-Renault, R.; Badré, S.; Galmiche, L.; Tang, J.; Audebert, P.; Clavier, G. *Eur. J. Org. Chem.* **2009**, 6121−6128.
(15) Montierth, J. M.; DeMario, D. R.; Kurth, M. J.; Schore, N. E. *Tetrahedron* **1998**, *54*, 11741−11748.
(16) Berréhar, J.; Lapersonne-Meyer, C.; Schott, M.; Weiser, G. *Chem. Phys.* **2004**, *303*, 129−136.
(17) Lauher, J. W.; Fowler, F. W.; Goroff, N. S. *Acc. Chem. Res.* **2008**, *41*, 1215−1229.
(18) Batchelder, D.N.; Bloor, D. Resonance Raman Spectroscopy of Conjugated Macromolecules. In *Advances in Infrared and Raman Spectroscopy*; Clark, R. J. H. , Hester, R. E., Eds.; Wiley Heyden: Chichester, U.K., 1984; Vol. *2*.
(19) Schott, M. *J. Phys. Chem. B* **2006**, *110*, 15864−15868.
(20) Batchelder, D. N.; Bloor, D. *J. Polym. Sci. : Polym. Phys. Ed.* **1979**, *17*, 569−581.
(21) Spagnoli, S.; Fave, J.-L.; Schott, M. *Macromolecules* **2011**, *44*, 2613−2625.
(22) Audebert, P.; Miomandre, F.; Clavier, G.; Vernière, M. C.; Badré, S.; Réallet-Renault, R. *Chem.—Eur. J.* **2005**, *11*, 5667−5673.
(23) Lécuiller, R.; Berréhar, J.; Lapersonne-Meyer, C.; Schott, M. *Chem. Phys. Lett.* **1999**, *314*, 255−260.
(24) Kobayashi, T. *J. Lumin.* **1992**, *53*, 159.